The International Journal of Cardiovascular Imaging (2022) 38:1555–1568
https://doi.org/10.1007/s10554-022-02543-w

ORIGINAL PAPER

Exploring myocardial fibrosis in severe aortic stenosis: echo, CMR and histology data from FIB-AS study

Giedrė Balčiūnaitė[1] · Justinas Besusparis[1] · Darius Palionis[1] · Edvardas Žurauskas[1] · Viktor Skorniakov[1] · Vilius Janušauskas[1] · Aleksejus Zorinas[1] · Tomas Zaremba[1,2] · Nomeda Valevičienė[1] · Pranas Šerpytis[1] · Audrius Aidietis[1] · Kęstutis Ručinskas[1] · Peter Sogaard[1,2] · Sigita Glaveckaitė[1]

Received: 8 December 2021 / Accepted: 25 January 2022 / Published online: 3 March 2022

Abstract

Myocardial fibrosis in aortic stenosis is associated with worse survival following aortic valve replacement. We assessed myocardial fibrosis in severe AS patients, integrating echocardiographic, cardiovascular magnetic resonance (CMR) and histological data. A total of 83 severe AS patients (age 66.4 ± 8.3, 42% male) who were scheduled for surgical AVR underwent CMR with late gadolinium enhancement and T1 mapping and global longitudinal strain analysis. Collagen volume fraction was measured in myocardial biopsies (71) that were sampled at the time of AVR. Results. CVF correlated with imaging and serum biomarkers of LV systolic dysfunction and left side chamber enlargement and was higher in the sub-endocardium compared with midmyocardium ($p<0.001$). CVF median values were higher in LGE-positive versus LGE-negative patients [28.7% (19–33) vs 20.7% (15–30), respectively, $p=0.040$]. GLS was associated with invasively (CVF; r=−0.303, $p=0.013$) and non-invasively (native T1; r=−0.321, $p<0.05$) measured myocardial fibrosis. GLS and native T1 correlated with parameters of adverse LV remodelling, systolic and diastolic dysfunction and serum biomarkers of heart failure and myocardial injury. Conclusion. Our data highlight the role of myocardial fibrosis in adverse cardiac remodelling in AS. GLS has potential as a surrogate marker of myocardial fibrosis, and high native T1 and low GLS values differentiated patients with more advanced cardiac remodelling.

Keywords Aortic stenosis · Myocardial fibrosis · Cardiovascular magnetic resonance · T1 mapping · Global longitudinal strain

Abbreviations

6MWT	6-Minute walking test
AS	Aortic stenosis
AV	Aortic valve
AVR	Aortic valve replacement
BNP	Brain natriuretic peptide
CAD	Coronary artery disease
CMR	Cardiovascular magnetic resonance
ECG	Electrocardiography
ECV	Extracellular volume
GLS	Global longitudinal strain
Hs-Tn-I	High-sensitivity troponin I
LA	Left atrium
LGE	Late gadolinium enhancement
LV	Left ventricle
LVEF	Left ventricular ejection fraction
MLHFQ	Minnesota Living With Heart Failure Questionnaire
NYHA	New York Heart Association
STE	Speckle tracking echocardiography

✉ Giedrė Balčiūnaitė
dr.giedre.balciunaite@gmail.com

[1] Present Address: Vilnius University: Vilniaus Universitetas, Vilnius, Lithuania

[2] Aalborg University Hospital, Clinical Institute of Aalborg University, Hobrovej 18-22, 9100 Aalborg, Denmark

Introduction

Myocardial fibrosis is fundamental in the pathogenesis of heart failure in the spectrum of cardiovascular diseases [1]. It is associated with the disruption of normal myocardial structure by excessive deposition of the extracellular matrix and creates a mechanistic base for adverse cardiac remodelling [2]. Myocardial fibrosis in aortic stenosis (AS) patients

has been linked to impaired left ventricular (LV) function and adverse clinical outcomes [3].

Changes in cellular and extracellular matrix architecture, triggered by the greater afterload and wall stress in AS, increases tissue stiffness and impairs contraction [4, 5]. This complex interplay between components of cardiac remodelling can be evaluated by histological analysis of myocardial biopsy samples or the use of advanced imaging techniques with ability of tissue characterization.

Cardiovascular magnetic resonance (CMR), strengthened by the development of T1 mapping, provides a non-invasive and global estimation of myocardial fibrosis. Two distinct types of myocardial fibrosis can be depicted by CMR: the late gadolinium enhancement (LGE) technique quantifies focal fibrosis [6, 7], and diffuse interstitial expansion can be measured by T1 mapping [8]. Multicentre trials and meta-analyses have shown that the presence and extent of LGE are predictors of worse survival following aortic valve replacement (AVR), indicating advanced myocardial injury [9, 10]. Focal myocardial fibrosis is also irreversible following AVR [11, 12], effecting incomplete recovery of LV function and worse post-operative clinical outcomes, suggesting delayed timing of aortic valve intervention in some patients.

Several studies in AS patients have reported that native T1 and extracellular volume (ECV) values correlate with the degree of diffuse myocardial fibrosis, predict cardiovascular events and mortality [13–15] and are reversible with afterload relief [16], demonstrating potential as an early marker of adverse remodelling.

As a possible surrogate marker of myocardial fibrosis, LV myocardial global longitudinal strain (GLS), as assessed by speckle tracking echocardiography (STE), has been shown to be an independent predictor of adverse events in patients with severe AS, both with preserved and impaired LV systolic function [17].

Thus, novel diagnostic strategies and more accurate evaluations of the disease severity and consequences of AS are needed in assessing subclinical myocardial dysfunction to further risk-stratify severe AS patients. There are limited studies on myocardial fibrosis that have integrated multimodality imaging and sufficient histological analyses in severe AS. The optimal T1 image analysis strategy remains debated, requiring further validation. Our prospective study aims to: (i) non-invasively assess markers of myocardial fibrosis and validate them against histological data in patients who are undergoing surgical AVR and (ii) identify early imaging biomarkers of adverse LV remodelling in severe AS patients.

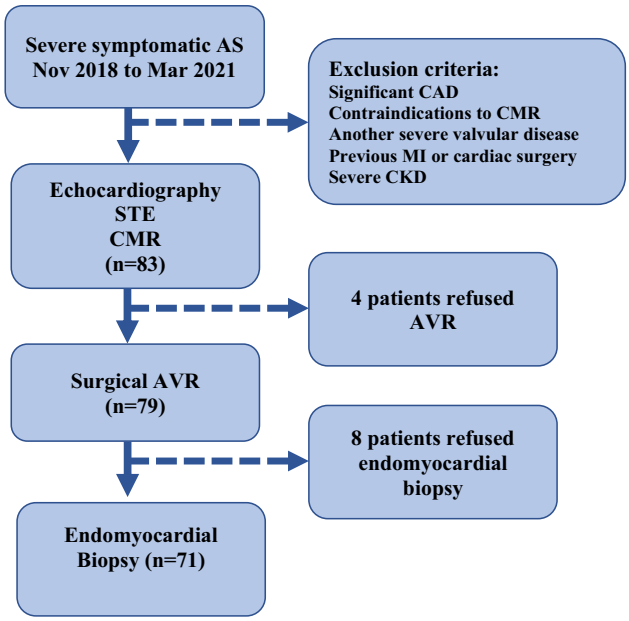

Fig. 1 FIB-AS study flow chart

Methods

Study population and protocol

In this prospective observational study at Vilnius University Hospital between November 2018 and December 2020, patients with severe symptomatic AS that were scheduled for AVR according to current treatment recommendations [18] were recruited. The study was approved by the Biomedical Research Ethics Committee of the Vilnius Region (Approval Number: 158200-18/9-1014-558) and was performed as part of the FIB-AS study (NCT03585933). This study conformed to the principles of the Helsinki Declaration, and all subjects gave written consent to participate.

Patients were recruited prior to a pre-operative assessment and underwent a clinical assessment, comprising a clinical history, the Minnesota Living with Heart Failure Questionnaire (MLHFQ), the 6-min walking test (6MWT), blood sampling [for haematocrit, renal function, brain natriuretic peptide (BNP) and high sensitivity troponin I (Hs-Tn-I)], a transthoracic echocardiogram, and CMR. The inclusion criteria were patients who were undergoing AVR for severe AS [defined as aortic valve area (AVA) ≤ 1 cm^2 or AVA index ≤ 0.6 cm^2/m^2, as determined by ultrasonography], age > 18 years, ability to undergo a CMR scan, and consent to the study protocol. The exclusion criteria were

significant coronary artery disease (CAD) (> 50% lesion), history of myocardial infarction, severe valve disease other than AS, estimated glomerular filtration rate < 30 mL/min/1.73 m^2, CMR-incompatible devices, persistent atrial tachyarrhythmias, and previous cardiac surgery (Fig. 1). The study data were collected and stored in a dedicated online database, REDCap (Research Electronic Data Capture) [19].

Cardiac imaging

Echocardiography

Transthoracic 2D echocardiography was performed using a commercially available Vivid ultrasound system (S70, E9 or E95) (GE Healthcare, Horten, Norway), and the data were stored on a dedicated workstation for subsequent off-line analysis. AS severity and LV systolic and diastolic function were evaluated per the echocardiographic guidelines [20, 21]. AVA was calculated using the continuity equation.

The 2D speckle tracking echocardiography (STE)

From the 2D grey-scale images of the apical 2-, 3- and 4-chamber views, LV global longitudinal strain (GLS) was measured and processed off-line using commercially available software (EchoPac 112.0.1, GE Medical Systems, Horten, Norway) [22]. The frame rate was adjusted to 50 to 80 frames/s. End-systole was defined, based on the closure click on the spectral tracing of the pulsed-wave Doppler of AV flow. GLS was acquired using the average regional strain curves (17-segment model for 2D STE). Segments with poor quality tracking or aberrant curves (despite manual adjustment) were removed from analysis. Due to missing data or poor image quality, STE analysis was completed for 77 of 83 patients.

CMR Protocol

CMR scans were obtained using standard protocols on a 1.5 T Siemens Aera scanner with surface coils and retrospective electrocardiography (ECG) triggering. LV end-systolic and end-diastolic diameters and maximum wall thickness were traced and recorded from the short-axis and long-axis views of the standard ECG-gated steady-state-free precession cine sequence. LV volumes, mass and ejection fraction were measured using commercial software (suiteHEART®) from a stack of sequential 8-mm short-axis slices (0–2-mm gap) from the atrio-ventricular ring to the apex. Measurements were indexed to body surface area in m^2 (using the DuBois formula).

LGE Imaging

To detect late gadolinium enhancement, images were acquired 10–15 min after intravenous administration of gadobutrol (0.2 mmol/kg) (Gadovist, Bayer AG, Germany) using a breath-hold segmented inversion recovery fast-gradient echo sequence in the short-axis and long-axis planes of the LV, with an 8-mm slice thickness and 0% distance factor. The region of myocardial fibrosis was defined as the sum of pixels with a signal intensity above 5 standard deviations of the normal remote myocardium in each short-axis slice. The presence of LGE was determined qualitatively by two independent readers who were blinded to the clinical data.

T1 Mapping

Myocardial fibrosis was assessed using native and post contrast T1 mapping at a mid-ventricular short-axis section, acquired using a modified Look-Locker inversion-recovery (MOLLI) sequence with motion correction (the '3–3-5'standard protocol) before and 15 min after contrast administration [23]. Scanner generated T1 maps were processed off-line using commercially available software (suiteHEART by NeoSoft). The region of interest was manually traced on short-axis, native and post-contrast T1 maps in the septum at the mid-ventricular level. All T1-related measures were traced in the middle third of myocardium to avoid partial volume effects. Segments containing LGE were excluded from the T1 mapping analysis [24]. To measure the T1 value

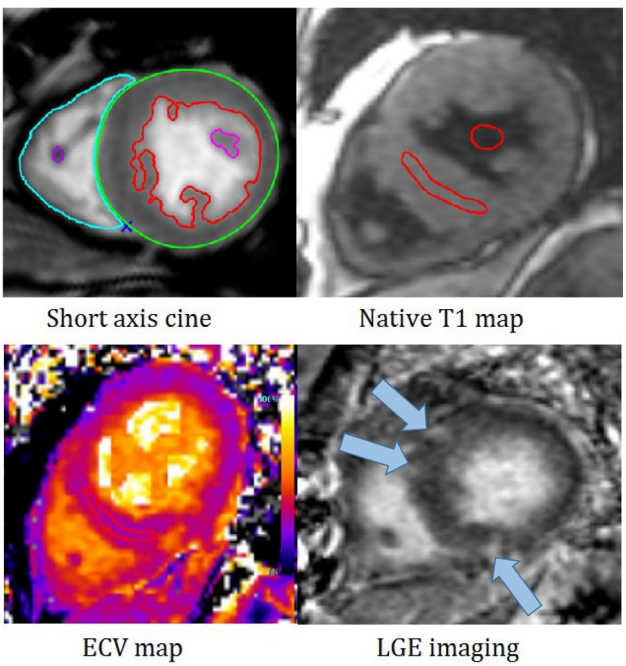

Fig. 2 Multiparametric CMR assessment protocol

of blood, circular regions of interest were positioned in the LV cavity, avoiding papillary muscle (Fig. 2). Native T1, ECV%, and indexed ECV values were then calculated. The ECV of the myocardium was calculated as follows: ECV% = (ΔR1m/ΔR1b) × (1—haematocrit level) × 100, where R1 is 1/T1, R1m is R1 in the myocardium, R1b is R1 in the blood and ΔR1 is the change in relaxation [25]. Hematocrit was drawn on the day of CMR scanning. Due to incomplete datasets, T1 mapping parameters were measured in 67 of 83 patients.

Histological analysis

At the time of surgical AVR, biopsy specimens were obtained under direct vision by the surgical team using a surgical scalpel from the basal anteroseptum just after removal of the diseased AV. One intraoperative myocardial biopsy sample (mean area 22.5 ± 12 mm^2) was taken from each patient. All myocardial tissue samples were fixed in 10% neutral buffered formalin and embedded in paraffin. Sections (3-µm-thick) were sliced on a Leica RM2145 microtome and stained with haematoxylin and eosin and Masson 's trichrome. Digital images were captured by on an Aperio Scan-Scope XT Slide Scanner (Aperio Technologies, Vista, CA, USA) under 20 × objective magnification (0.5 µm resolution). Histologists who were blinded to the clinical and CMR data examined all biopsy specimens.

The fraction of myocardial volume that was occupied by collagen tissue (collagen volume fraction, CVF) was determined by quantitative morphometry on an automated image analysis system (HALO™). The area of myocardial fibrosis was calculated using the HALO™ Area Quantification v2.1.11 algorithm (IndicaLabs, NM, USA) [26]. The subendocardial layer was defined as 1 mm from the endocardial surface, whereas the rest of the tissue sample was defined as the midmyocardial layer.

Statistical analysis

Variables were presented as mean ± standard deviation or median and interquartile ranges. Categorical variables were expressed as frequencies and percentages and were compared by v2 test. Unpaired student's t-test and Mann–Whitney U test were used to compare two groups of continuous variables. Pearson's and Spearman's correlation coefficients were calculated to assess the relationships between continuous variables.

Intra- and inter-observer variation was analysed by Bland–Altman method and calculation of the correlation coefficient. The statistical analysis was performed in R (version 4.1.2). Differences were considered statistically significant provided a 2-sided p value < 0.05 [27].

Results

A total of 83 patients were included (age 66.4 ± 8.3 years, 58% female, AVA index 0.44 ± 0.1 cm^2/m^2, peak AV velocity 4.8 ± 0.6 m/s, mean gradient 57.8 ± 16 mm Hg). The main reasons for non-eligibility were significant CAD, renal dysfunction and other valvular abnormalities. The mean LV ejection fraction (LVEF) was 66.8 ± 13%, with 11% of patients having reduced LVEF (< 50%). Overall, patients had low surgical risk, with STS-PROM and EuroScore < 4% (1.9% and 1.5%, respectively). Patients with congenital AS were more likely to be younger ($p < 0.001$), were at lower surgical risk ($p = 0.004$), and had better renal function ($p = 0.002$). Of the 83 enrolees, 79 underwent surgical AVR and 4 postponed surgery due to Covid-19. The patients' clinical and imaging characteristics are summarised in Tables 1 and 2.

Myocardial fibrosis by histology

Of 71 myocardial biopsies, 2 were epicardial. The data of one patient was excluded from the analysis due to an incidental finding of toxoplasmic myocarditis. The median CVF was 15.1% (8.6–21). Patients with higher CVF had a greater prevalence of hypertension ($p = 0.024$) and dyslipidaemia ($p = 0.036$). Higher values of CVF were observed in LGE-positive versus LGE-negative patients—28.7% (19–33) vs 20.7% (15–30), respectively ($p = 0.040$). No significant differences in median CVF value were noted between patients with and without CAD [17.2% (10–23) vs 13.4% (9–19), respectively; $p = 0.094$]. Segmental analysis of myocardial biopsies revealed more fibrosis in the subendocardial layer compared with a midmyocardial layer [21.1% (12–29) vs 8% (5–12); $p < 0.001$; Fig. 3).

Myocardial fibrosis by CMR

The median delay between CMR and surgery was 53.3 days (17–78). Mean native T1 was 959.7 ± 34 ms (range: 897–1044 ms), and the mean ECV was 22.7 ± 3.6% (range: 15.7–34.4%). No significant difference in mean native T1 and ECV values was observed between men and women (962 ± 29 ms vs 957 ± 37 ms, $p = 0.391$ and 22.9 ± 3% vs. 22.6 ± 4%, $p = 0.821$, respectively).

To compare native T1 with clinical and structural parameters, we divided variables (above and below the median: 957 ms, Table 3). Patients with elevated native T1 had lower systolic blood pressure ($p = 0.006$), higher QRS voltage on the ECG ($p = 0.036$), greater systolic ($p = 0.009$) and diastolic LV dimensions ($p = 0.049$) and higher LV mass index ($p = 0.021$). Among those with elevated native T1, a higher

Table 1 Clinical characteristics of the study population stratified by the presence of focal fibrosis

Variable	All patients ($n=83$)	LGE (+) patients ($n=61$)	LGE (-) patients ($n=22$)	*P*- value
Age, yrs	66.4 ± 8.3	65.8 ± 8.3	68.3 ± 8.3	0.235
Male gender	35 (42%)	29 (48%)	6 (27%)	0.162
BMI, kg/ m^2	30 ± 5.8	30.4 ± 5.6	28.7 ± 6	0.245
BSA, m^2	1.9 ± 0.2	2.0 ± 0.2	1.8 ± 0.2	**0.011**
Systolic BP, mmHg	150 ± 25	148 ± 25	156 ± 23	0.223
Diastolic BP, mmHg	85 ± 11	84 ± 12	85 ± 11	0.842
Comorbidities				
Hypertension	73 (88%)	55 (90%)	19 (86%)	0.732
Dyslipidemia	66 (80%)	48 (79%)	19 (86%)	0.640
Unobstructive CAD	39 (47%)	30 (49%)	9 (41%)	0.677
Diabetes mellitus	14 (17%)	10 (16%)	5 (22%)	0.735
Atrial fibrillation	6 (7%)	5 (8%)	1 (5%)	0.931
History of PCI	1 (1%)	1 (2%)	-	1.000
Symptoms and functional status				
Dyspnea	61 (74%)	46 (75%)	15 (68%)	0.706
Chest pain	41 (49%)	30 (49%)	11 (50%)	1.000
Syncope	9 (11%)	9 (15%)	-	0.131
NYHA functional class				0.591*
I	16 (19%)	11 (18%)	5 (23%)	
II	24 (29%)	19 (31%)	5 (23%)	
III	40 (48%)	28 (46%)	12 (54%)	
IV	3 (4%)	3 (5%)	-	
6 MWT, m	357.6 ± 105.6	352 ± 108	372 ± 101	0.459
MLHFQ score	35 ± 20.4	36 ± 20	31 ± 22	0.277
Drug history				
ACE-I/ARB	61 (74%)	43 (71%)	18 (82%)	0.453
Betablocker	57 (69%)	42 (69%)	15 (68%)	1.000
Statin	54 (65%)	40 (66%)	14 (64%)	1.000
Loop diuretic	15 (18%)	11 (18%)	4 (18%)	1.000
Spironolactone	22 (27%)	14 (23%)	8 (36%)	0.347
Risk scores				
STS-PROM, %	1.9 (1.2–2.3)	1.6 (1–2.2)	1.75 (1.4–2.4)	0.415
EuroSCORE II, %	1.5 (0.7–1.6)	1 (0.7–1.7)	1.2 (0.8–1.5)	0.415
Surgery (n = 79)				
Tissue valve	70 (89%)	55 (90%)	15 (83%)	**0.037**
Mechanical valve	9 (11%)	6 (10%)	3 (17%)	0.927
Aortic intervention	3 (4%)	1 (2%)	2 (11%)	0.348
Valve morphology				
Tricuspid	54 (65%)	41 (67%)	13 (59%)	0.671
Bicuspid	28 (34%)	19 (31%)	9 (41%)	0.429
Unicuspid	1 (1%)	1 (2%)	–	1.000
Blood tests				
Creatinine µmol/l	76.2 ± 16.3	77 ± 17	73.9 ± 16	0.447
eGFR, ml/min/1.73 m^2	78.6 (69–90)	85 (69–90)	86 (69–90)	0.996
Hs-Tn-I, pg/l	10 (5–19)	13.5 (6–29)	5.3 (5–9)	**0.003**
BNP, pg/l	122 (65–340)	167 (77–511)	74 (43–145)	**0.004**
ECG parameters				
Heart rate, beats/min	77 ± 12.4	78 ± 12	76 ± 13	0.519
S-L criteria (mm)	30.8 ± 10	31.7 ± 10	28.4 ± 10	0.189

Table 1 (continued)

Variable	All patients ($n=83$)	LGE (+) patients ($n=61$)	LGE (-) patients ($n=22$)	*P*- value
QRS duration, ms	96.8 (88–102)	94 (88–102)	92 (85–101)	0.449

The boldface values indicate statistical significance

Continuous variables are presented as mean ± SD or median [interquartile range]. Categorical variables are expressed as n (%)

6 MWT 6 min walking test, *BMI* Body mass index, *BNP* Brain natriuretic peptide, *BP* Blood pressure, *BSA* Body surface area, *CAD* Coronary artery disease, *ECG* Electrocardiography, *LGE* Late gadolinium enhancement, *MLHFQ* Minnesota living with heart failure questionnaire, *NYHA* New York Heart Association, *PCI* Percutaneous coronary intervention, *S-L* Sokolow Lyon voltage criterion, *STS* Society of Thoracic Surgeons' risk model score, *EuroScoreII* European System for Cardiac Operative Risk Evaluation II score, *ACE-I* Angiotensin-converting-enzyme inhibitor, *ARB* Angiotensin-receptor blocker, *hs-Tn-I* High sensitivity troponin I, *eGFR* Estimated glomerular filtration rate

*-*P*-value for comparison among NYHA I and II vs. III and IV

proportion of patients had reduced GLS (18% vs 6%, respectively; $p=0.049$).

Focal fibrosis, measured by LGE, was common, affecting 74% of all patients (83% of men and 67% of women). Further, 92% of focal fibrosis was the non-infarct type (89% mid-myocardial, 3% subepicardial). Despite having unobstructed coronary arteries 8% of patients had infarct-type focal fibrosis. The most common location of LGE was the right ventricular insertion point (68%). LGE was also detected in the anterolateral (11%), septal (8%), posterolateral (6%), inferior (6%) and apical (1%) segments. We found no significant difference in the prevalence of LGE between patients with and without CAD (77% and 70%, respectively; $p=0.67$). Compared with patients without focal fibrosis, LGE-positive subjects had more severe AS, as evidenced by smaller AVA index ($p=0.018$), thicker LV walls ($p<0.001$) and higher LV mass index ($p=0.009$). Patients with LGE also had higher levels of BNP ($p=0.004$) and Hs-Tn-I ($p=0.003$). The patients' clinical and imaging characteristics stratified by the presence of LGE are summarised in Tables 1 and 2.

Longitudinal deformation analysis

The mean GLS was $-18\pm5\%$ (range: -3% to -31%), and a reduction in GLS > -20% was observed in 61% of patients.

To analyse GLS with regard to clinical and structural parameters, we dichotomised the variables (above and below median: -18.5%; Table 3). Patients with lower GLS had more severe AS, based on smaller AVA index ($p=0.018$), higher mean transvalvular gradient ($p=0.004$), lower systolic blood pressure ($p=0.005$) and greater QRS voltage on the ECG ($p=0.011$). The low-GLS group also had thicker LV walls ($p=0.009$), higher LV volumes ($p<0.001$), greater LV mass index ($p<0.001$) and lower LVEF ($p<0.001$). This group showed signs of elevated LV filling pressures, as evident by higher E/e' ratios ($p=0.011$), with consequently higher LA volume index ($p=0.002$) and pulmonary artery systolic pressure (p = 0.031). Higher levels of BNP ($p=0.001$) and Hs-Tn-I ($p=0.002$) were detected in these patients. Representative images of patients with various degrees of LV remodelling by echocardiography, CMR and histology are shown in Fig. 4.

Analysis of associations

CVF correlated with LV end-diastolic diameter (r = 0.242, $p=0.043$), LV end-systolic volume (r = 0.265, $p=0.028$), LVEF (r = −0.246, $p=0.04$) and LA volume index (r = 0.314, $p=0.009$). When subendocardium was excluded from the analysis, CVF correlated with LV mass (r = 0.247, $p=0.041$), LVEF (r = −0.354, $p=0.003$), GLS (r = −0.303, $p=0.013$) and BNP (r = 0.242, $p=0.045$) (Fig. 5). Native T1, ECV and indexed ECV did not associate with CVF.

With regards to LV structure and function, GLS correlated with LV end-diastolic volume (r = −0.485, $p<0.001$), LV end-systolic volume (r = −0.636, $p<0.001$), LV mass index (r = −0.615, $p<0.001$) and LVEF (r = 0.7, $p<001$). GLS was also linked to parameters that were associated with elevated LV filling pressures: mean E/e' (r = −0.4, $p=0.002$), LA volume index (r = −0.405, $p<0.001$) and estimated pulmonary artery systolic pressure (r = −0.376, $p<0.05$). Native T1 correlated with LV end-systolic volume (r = 0.349, $p=0.003$), LV end-diastolic volume (r = 0.269, $p=0.03$), LV mass index (r = 0.414, $p<0.001$) and LVEF (r = 0.317, $p<0.05$). GLS and native T1 were associated with the degree of AS severity: AV mean gradient (r = −0.387, $p<0.001$ and r = 0.408, $p<0.001$, respectively) and AVA (r = 0.30, $p<0.05$ and r = 0.3, $p=0.02$, respectively).

With regard to serum biomarkers, GLS and native T1 correlated with BNP (r = −0.653, $p<0.001$ and r = 0.371, p < 0.05, respectively) and hs-Tn-I (r = −0.486, $p<0.001$

Table 2 Cardiovascular imaging and histology data of study cohort, stratified by the presence of focal fibrosis

Echocardiography data ($n=83$)	All patients ($n=83$)	LGE (+) patients ($n=61$)	LGE (-) patients ($n=22$)	P-value
Peak AV velocity, m/s	4.8 ± 0.6	4.9 ± 0.6	4.6 ± 0.5	0.074
Mean AV gradient, mm Hg	57.8 ± 16	59.8 ± 17	52.4 ± 14	0.071
Low gradient AS	10 (12%)	6 (10%)	4 (18%)	0.422
AVA, cm^2	0.84 ± 0.2	0.83 ± 0.2	0.88 ± 0.2	0.364
AVA index, cm^2/ m^2	0.44 ± 0.1	0.43 ± 0.1	0.49 ± 0.1	**0.018**
IVSd, mm	12.7 ± 1.7	13.1 ± 1.5	11.5 ± 1.5	**< 0.001**
Posterior wall diameter, mm	11.5 ± 1.4	11.9 ± 1.3	10.3 ± 1.2	**< 0.001**
LVdd, mm	51.4 ± 5.4	52.1 ± 5.4	49.3 ± 4.9	**0.034**
LVsd, mm	32.7 ± 5.9	33.1 ± 6.1	31.7 ± 5.6	0.362
E/A	1.1 ± 0.5	1.1 ± 0.5	1.2 ± 0.3	0.615
E deceleration time, ms	259 ± 70	257 ± 69	262 ± 74	0.813
E/e' septal	17.6 ± 7	17.9 ± 6.3	16.8 ± 9.5	0.619
E/e' lateral	14.5 ± 6	15 ± 6.5	13.2 ± 5.8	0.276
E/e' mean	15.6 ± 6	16 ± 5.9	14.3 ± 5.7	0.254
LA volume index, ml/ m^2	47.9 ± 12	49.2 ± 12	44.7 ± 12	0.129
PASP, mm Hg	38 ± 15	40.5 ± 15	33.6 ± 12	0.175
RV S', cm/s	11.6 ± 3	11.4 ± 3	12 ± 2	0.377
TAPSE	21.7 ± 3	21.7 ± 4	21.8 ± 3	0.924
GLS, %*	−18 ± 5	−17.5 ± 4.8	−19.4 ± 5.3	0.147
CMR data (n = 83)				
IVSd, mm	13.3 ± 2	13.6 ± 2	12.6 ± 2	0.062
LVdd, mm	50.6 ± 6	51 ± 6	49.3 ± 6	0.264
LVsd, mm	33.8 ± 8	34.2 ± 8	33 ± 9	0.561
LVEDV, ml	144.3 ± 44	149.7 ± 44	130 ± 44	0.079
LVESV, ml	51 (28- 61)	46 (31–69)	29 (24–45)	0.106
LV stroke volume index, ml/m^2	48 ± 11	48.3 ± 10	48.4 ± 11	0.982
LVEF, %	66.8 ± 13	65.3 ± 13	70.8 ± 12	0.088
LVEF < 50%	9 (11%)	8 (13%)	1 (5%)	0.427
LV mass index, g/m^2	97.6 ± 32	103.4 ± 32	82.6 ± 29	**0.009**
RVEDV, ml	125.3 ± 31	129.5 ± 31	114.2 ± 31	0.052
RVESV, ml	49.3 ± 18	49.7 ± 19	48.3 ± 17	0.747
RVEF, %	60.8 ± 10	61.9 ± 10	58 ± 8	0.111
Native T1, ms#	959.7 ± 34	961.8 ± 31	952.5 ± 43	0.359
Post-contrast T1, ms#	351 (326- 362)	361 (325–376)	350 (326–358)	0.415
ECV, %#	22.7 ± 3.6	23.4 ± 3.7	22.2 ± 3.5	0.541
ECV index, $\%/m^2$	11.8 ± 2	12.3 ± 2	11.3 ± 2	0.271
Histology data (n = 71)				
CVF, %&	15.1 (9–21)	15.9 (9–19)	12.4 (9–24)	0.887
CVF subendocardial, %&	21.1 (12–29)	28.7% (19–33)	20.7% (15–30)	**0.040**

The boldface values indicate statistical significance

Continuous variables are presented as mean ± SD or median [interquartile range]. Categorical variables are expressed as *n* (%)

AV Aortic valve, *AVA* Aortic valve area, *E* Peak early velocity of the transmitral flow, *CMR* Cardiovascular magnetic resonance, *CVF* Collagen volume fraction, *e'* Peak early diastolic velocity of the mitral annulus displacement, *GLS* Global longitudinal strain, *ECV* Extracellular volume, *IVSd* Interventricular septum diastolic diameter, *LVEDV* Left ventricular end-diastolic volume, *LVESV* Left ventricular end-systolic volume, *LVEF* Left ventricular ejection fraction, *LA* Left atrium, *LGE* Late gadolinium enhancement, *LGE(+)* Patients with late gadolinium enhancement, *LGE(-)* Patients without late gadolinium enhancement, *PASP* Pulmonary artery systolic pressure measured by echocardiography, *RVEDV* Right ventricular end-diastolic volume, *RVEF* Right ventricular ejection fraction, *RVESV* Right ventricular end-systolic volume, *RV S'* Peak systolic velocity of the tricuspid annulus displacement, *TAPSE* Tricuspid annulus plane systolic excursion, *- value based on the data analysis in 77 patients; #- values based on the data analysis in 67 patients; &- values based on the data analysis in 71 patient

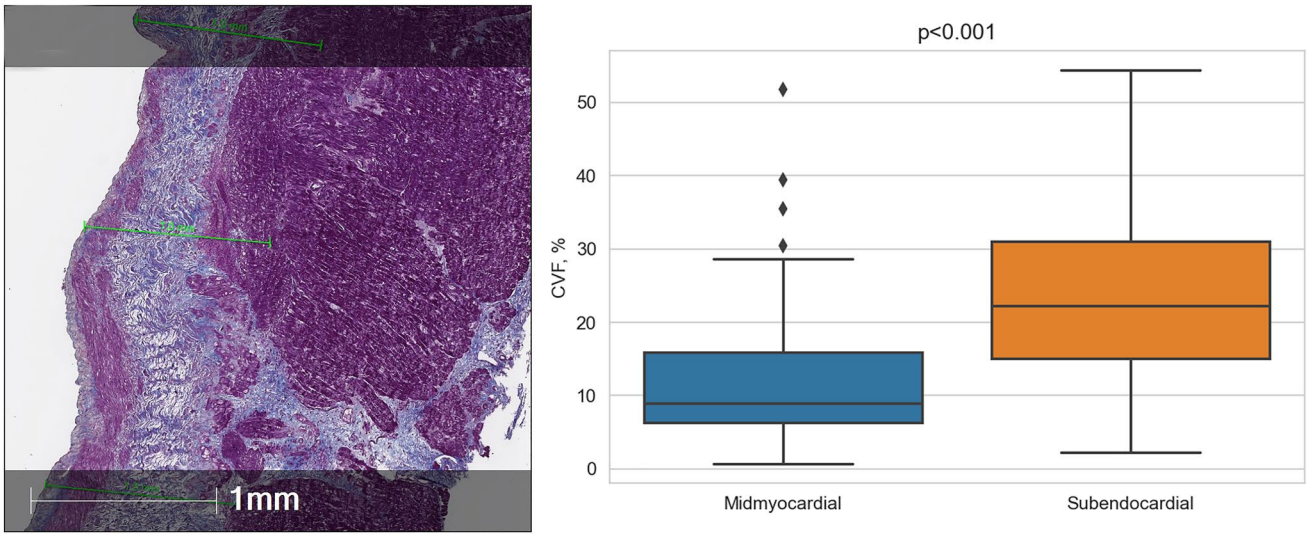

Fig. 3 Image on the left shows myocardial biopsy sample stained with Masson 's trichrome. Graph on the right shows comparison of collagen volume fraction (CVF) in different layers of myocardium. Higher proportion of collagen detected in subendocardium compared to midmyocardium

and r = 0.333, $p < 0.05$, respectively) and with each other (r = −0.321, $p < 0.05$) (Fig. 6).

Reproducibility of measurements

The intraclass correlation coefficients for native T1 were 0.945 (95% CI 0.88–0.97, bias 3.3 ± 11.0 ms) for intra-observer variation and 0.958 (95% CI 0.91–0.98, bias 9.1 ± 15.1 ms) for inter-observer variation. The GLS measurements also demonstrated excellent reproducibility: 0.969 (95% CI 0.93–0.98, bias 0.51 ± 1.3) for intra-observer variation and 0.981 (95% CI 0.96–0.99, bias 1.5 ± 1) for inter-observer variation.

Discussion

This prospective study presents a comprehensive assessment of the consequences of AS on LV myocardium by integrating CMR and STE data with a large number of myocardial biopsies.

The main study findings are as follows:

(1) The non-infarct type of focal fibrosis is highly prevalent in severe low-risk AS patients and determines more advanced LV remodeling.
(2) Histologically measured myocardial fibrosis is associated with imaging and serum biomarkers of LV systolic dysfunction and left side chamber enlargement.
(3) The subendocardium is affected by myocardial fibrosis to a greater extent and determines longitudinal dysfunction.
(4) GLS is associated with invasively and non-invasively measured myocardial fibrosis; low GLS and elevated native T1 differentiated patients with more advanced LV remodelling.

Compared with previous studies in severe AS patients, our cohort was younger and free from significant CAD, thus representing low-risk isolated AS patients. Although 90% of our study population had preserved LVEF, a more detailed assessment of myocardial structure and function through cardiac imaging and histological analysis revealed evidence of varying degrees of myocardial injury.

The amount of fibrosis in the myocardial biopsies varied substantially, from 2% to 41%. Diffuse fibrosis, which is present in healthy myocardium, constituted less than 2%, based on the autopsy results of subjects who died of non-cardiovascular causes [28, 29]. If the amount of myocardial fibrosis increases with age is less clear. We found that histological myocardial fibrosis was associated with LV and LA enlargement and worse systolic function, underscoring the role of myocardial fibrosis in the pathophysiological progression to cardiac decompensation in AS, in terms morphology and function. Consistent with earlier studies, we found that the subendocardial layer contained more fibrosis compared with a midmyocardium. Gradients of myocardial fibrosis in the LV wall have been described in patients with severe AS and those with hypertrophic cardiomyopathy and hypertensive heart disease—conditions that are both

Table 3 Patients clinical and imaging characteristics stratified by median GLS and native T1 values

	GLS ≥ -18.5% ($n=40$)	GLS < -18.5% ($n=37$)	*P*-value	Native T1 ≥ 957 ms (n = 34)	Native T1 < 957 ms (n = 33)	*P*-value
Age, yrs	66 ± 8	68 ± 8	0.256	65.8 ± 9	66 ± 9	0.917
Male gender	18 (45%)	14 (38%)	0.548	15 (44%)	11 (33%)	0.446
BSA, m^2	1.98 ± 0.2	1.86 ± 0.2	**0.004**	1.96 ± 0.16	1.93 ± 0.19	0.607
Systolic BP, mmHg	143 ± 23	158 ± 23	**0.005**	139 ± 21	156 ± 26	**0.006**
Diastolic BP, mmHg	83 ± 11	85 ± 11	0.485	82 ± 10	86 ± 13	0.203
Unobstructive CAD	20 (50%)	18 (49%)	1.0	20 (59%)	14 (42%)	0.893
Hypertension	36 (90%)	33 (89%)	0.447	27 (79%)	33 (100%)	0.109
Diabetes mellitus	8 (20%)	4 (11%)	0.768	6 (18%)	7 (21%)	1.0
NYHA f.cl. ≥ 3	26 (65%)	14 (38%)	0.085	16 (47%)	15 (46%)	0.749
MLHFQ score	37 ± 20	32 ± 20	0.257	37 ± 21	36 ± 20	0.839
6 MWT, m	351 ± 105	358 ± 104	0.767	367 ± 106	352 ± 94	0.558
ECG						
HR, b/min	80 ± 14	75 ± 11	0.100	78 ± 4	77 ± 12	0.742
QRS, ms	95 (90–102)	90 (86–98)	0.105	94 (89–102)	90 (84–101)	0.313
S-L, mm	34 ± 11	28 ± 8.5	**0.011**	34 ± 10	29 ± 9	**0.036**
Echo data						
AVA index, cm^2/m^2	0.42 ± 0.1	0.47 ± 0.08	**0.018**	0.4 ± 0.1	0.45 ± 0.1	0.075
Peak AV velocity, m/s	5.0 ± 0.7	4.7 ± 0.5	0.055	5.0 ± 0.6	4.8 ± 0.6	0.105
Mean gradient, mmHg	63 ± 17.7	53 ± 13.2	**0.004**	64 ± 16	57 ± 15	0.052
IVSd, mm	13.3 ± 1.8	12.2 ± 1.4	**0.009**	13 ± 1.9	12.6 ± 1.6	0.368
LVdd, mm	53.7 ± 12	48.8 ± 4.7	**0.002**	53 ± 5	50 ± 5	**0.049**
LVsd, mm	35.4 ± 6	29.6 ± 4	**< 0.001**	35 ± 6	32 ± 6	0.057
E deceleration time, ms	254 ± 76	264 ± 67	0.542	252 ± 68	266 ± 75	0.759
E/e' septal	17.1 (14–22)	14 (11.7–18)	**0.011**	16.5 (12.8–18)	16 (12–20)	0.845
E/e' mean	17.4 ± 6.9	14.2 ± 4.4	**0.021**	15 ± 5	16 ± 7	0.909
LA volume index, ml/m^2	53 ± 12	44 ± 11	**0.002**	48 ± 9	48 ± 15	0.473
PASP, mmHg	43.5 ± 18	32.9 ± 7	**0.031**	41 ± 17	37 ± 12	0.947
GLS,%	14.3 ± 3.9	21.7 ± 2.7	**< 0.001**	16.7 ± 5.6	18.2 ± 4	0.120
GLS > -15%	16 (40%)	-	**< 0.001**	10 (29%)	4 (12%)	**0.049**
CMR and histology data						
IVSd, mm	14 ± 2	12.6 ± 2	**0.005**	14 ± 1.6	13 ± 2.3	0.364
LVdd, mm	53 ± 7	48.3 ± 5	**< 0.001**	52 ± 6	50 ± 5	0.074
LVsd, mm	37 ± 9	30.6 ± 6	**< 0.001**	36.5 ± 7	32 ± 6	**0.009**
LVEDV, ml	160.7 ± 48	126 ± 35	**< 0.001**	153 ± 40	143 ± 44	0.201
LVESV, ml	56.9 (41–77)	29 (24–41)	**< 0.001**	52 (37–72)	41 (28–53)	0.083
LVEF, %	59 ± 14	74 ± 7	**< 0.001**	62.4 ± 14	68 ± 12	0.053
LVEF < 50%	8 (20%)	0	**0.009**	6 (18%)	2 (6%)	0.541
LV mass index, g/m^2	113 ± 33	80.6 ± 24	**< 0.001**	109 ± 31	91 ± 30	**0.021**
LGE prevalence	34 (85%)	23 (62%)	0.058	27 (79%)	25 (76%)	0.802
Native T1, ms	967 ± 31	950 ± 37	0.066	987 ± 26	936 ± 18	**< 0.001**
Post-contrast T1, ms	349 (326–354)	355 (332–366)	0.201	352 (328–362)	348 (318–362)	0.445
ECV, %	22.3 ± 4	22.9 ± 2.4	0.456	23 ± 3.2	22 ± 3.9	0.243
T2, ms	43 (41–45)	42 (40–44)	0.196	43.3(41–45)	42(40–44)	0.291
BNP, pg/l	252 (98–813)	79 (59–173)	**0.001**	163 (73–581)	120 (62–260)	0.413
Hs-Tn-I, pg/l	15 (7.5–29)	6.9 (5–12.9)	**0.002**	14 (7–27)	7.5 (5–16)	0.089
CVF, %	17.2 (10–22)	13.5 (8–20)	0.279	18.1 (8–24)	13.4 (10–21)	0.564
CVF subendocardial,%	23.4 (13–33)	18.4 (11–27)	0.199	22.3 (9–28)	18.8 (12–26)	0.855

Continuous variables are presented as mean ± SD or median [interquartile range]. Categorical variables are expressed as n (%). The boldface values indicate statistical significance. Abbreviations as in Tables 1 and 2

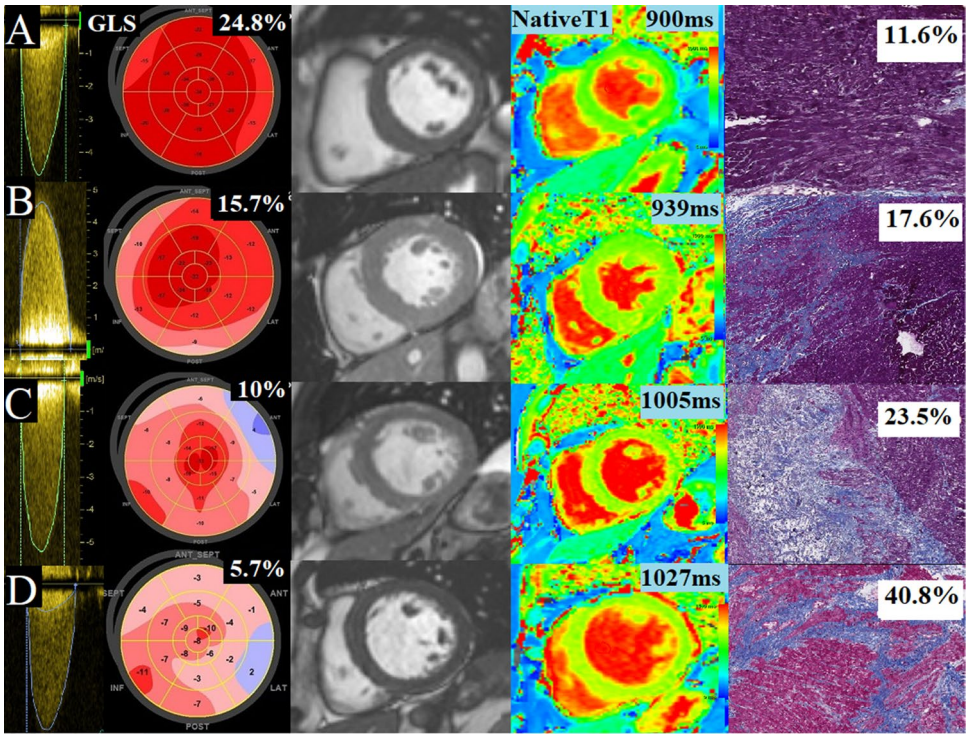

Fig. 4 Four exemplar patients showing progressive cardiac remodeling: continuous-wave Doppler (maximum velocities > 4 m/s; Column 1), global longitudinal strain (GLS; Column 2), short axis cine stills demonstrating degrees of left ventricular (LV) remodeling (Column 3), matching native T1 (Column 4) and collagen volume fraction (CVF) in myocardial biopsies stained with Masson 's trichrome (Column 5). Patient A has preserved GLS, minimal LV hypertrophy, low native T1 and CVF of 11.6%. Patient B has reduced GLS, concentric LV hypertrophy, higher native T1 and moderate histological fibrosis (CVF-17.6%). Patient C has low GLS, evidence of LV hypertrophy, high native T1 and significant histological fibrosis (CVF-23.5%). Patient D, with decompensated heart failure, has low GLS, LV cavity dilatation, high native T1 and extensive histological fibrosis (CVF-40.8%)

associated with chronic pressure overload and an increase in LV mass [28, 29]. These findings can be explained by a transmural gradient of wall stress and ischemia in the subendocardial layer due to the relative decrease in capillary density, with subsequent cell loss and reparative fibrosis [30].

GLS and native T1 median values differentiated patients with more advanced LV remodelling, wherein patients with lower GLS and higher native T1 had evidence of altered LV structure, diastolic and systolic impairments and higher levels of serum biomarkers, indicative of heart failure and myocardial injury. Notably, patients with reduced GLS and elevated native T1 still had preserved LVEF, and only 20% of patients with adverse structural and functional cardiac remodelling had LVEF below 50%. Thus, only 1 in 5 patients with advanced cardiac remodelling can be detected if only this echocardiographic criterion of cardiac decompensation is used, overlooking a substantial number of patients who would benefit from early AV intervention. Our results are consistent with previous studies, showing that fibrotic changes that are induced by AS begin in the subendocardium and initially affect longitudinal function, which is not well represented by LVEF, because it can be compensated by global radial function [7, 31].

Notably, patient groups did not differ by symptom status, functional capacity or quality of life assessment. This finding suggests that symptom assessments can be challenging and misleading and do not always reflect true cardiac condition, indicating that the decision to intervene should be supported by objective markers of cardiac injury, rather than based on subjective assessment of symptom status.

Imaging biomarkers, or the integration of several parameters, might be particularly useful in patients with no or minimal symptoms or when ascertaining valve-related symptoms is challenging. Our data implicate GLS and native T1 as early markers of cardiac decompensation. GLS can also be used as a surrogate marker of myocardial fibrosis, as it was associated with both, invasively and non-invasively measured myocardial fibrosis.

Seventy-four percent of our patients had areas of focal fibrosis, 98% of which were the non-infarct type and which were independent of the presence of nonobstructive CAD. Although only 1 or 2 segments were affected by LGE in most patients, data from a recent large multicentre study show that > 2% of

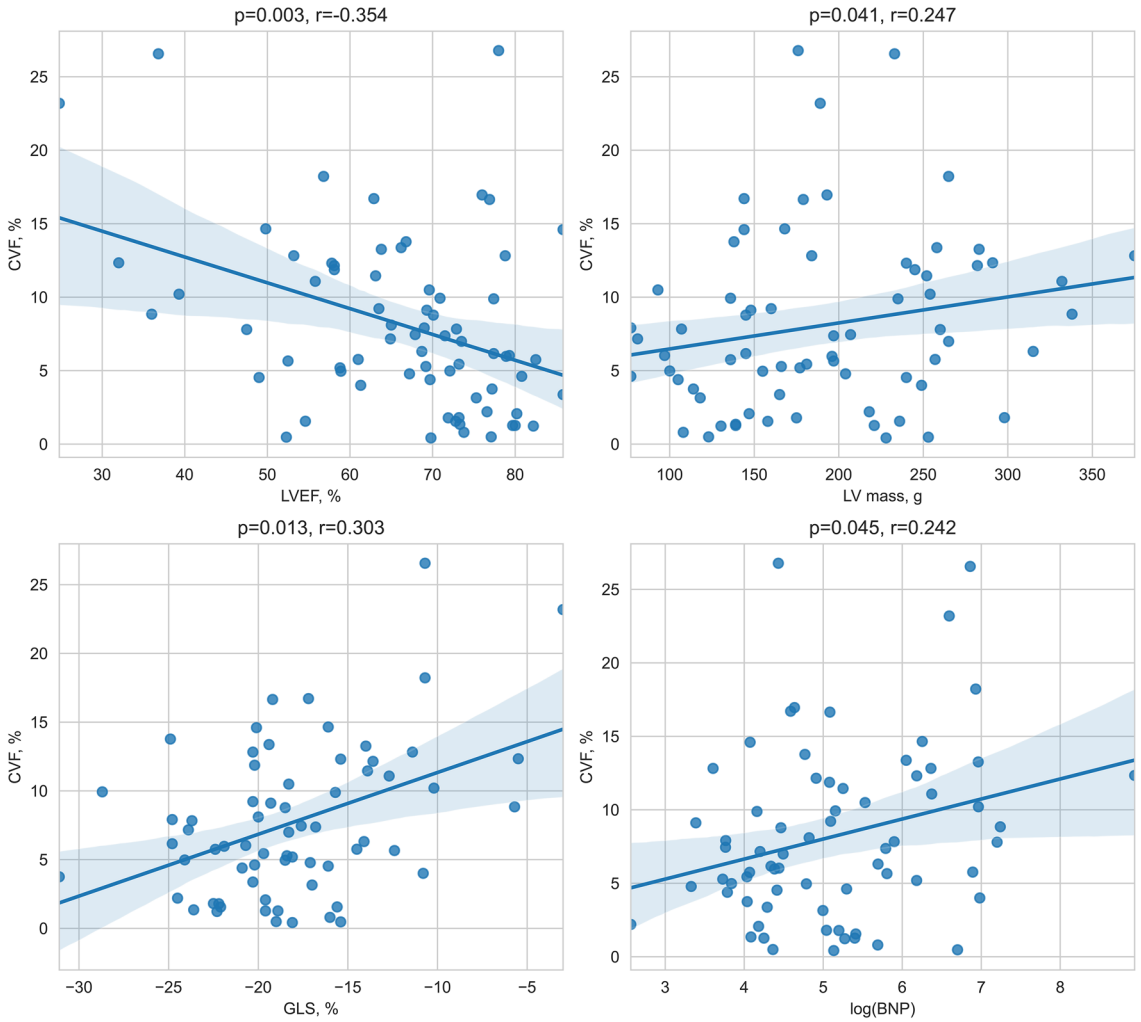

Fig. 5 Correlations between histological myocardial fibrosis (CVF) and LV ejection fraction (**a**), LV mass (**b**), GLS (**c**) and brain natriuretic peptide (BNP) (d) are shown. Abbrevations are as in Fig. 4

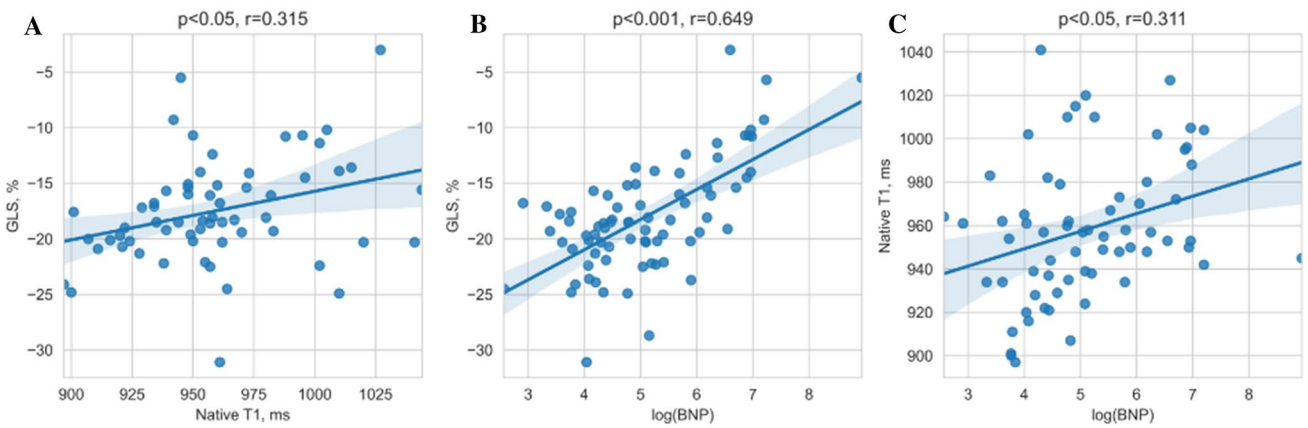

Fig. 6 Correlations between GLS and native T1 (**a**), GLS and BNP (**b**), native T1 and BNP (**c**) are shown. Abbrevations are as in Figs. 4 and 5

LGE in patients with severe AS who undergo AVR is associated with worse postoperative survival [32]. We found, that the myocardium of patients who have progressed to more advanced myocardial injury and have developed areas of irreversible replacement fibrosis on CMR also contains higher degree of diffuse fibrosis measured histologically. Unexpectedly, we found no associations between CVF and CMR markers of diffuse fibrosis, for which there are several explanations. There was a possible sampling error, because only 1 biopsy sample per patient was analysed. Further, the histological and T1 mapping analyses were performed at different levels and layers of the interventricular septum. The myocardial biopsies were endocardial and taken from the basal anteroseptum, possibly containing higher amounts of fibrotic tissue, and the region of interest for the T1 mapping measurements was drawn in the middle of the septum at the midventricular level, avoiding endo and epicardial borders. The data in this field are inconsistent, with some studies reporting significant associations between invasively and non-invasively measured myocardial fibrosis in AS cohorts [15, 33] and others failing to demonstrate this association [24, 29].

Although our patients presented with increased LV mass and myocardial fibrosis in the histological analysis, ECV values were not elevated in our cohort compared with our local reference range. This finding can be explained by the greater increase in cellular mass (adaptive hypertrophy), as opposed to the expansion of extracellular space, because ECV per se represents the percentage of space that is occupied by the extracellular compartment of the total LV mass. The average native T1 and ECV values in our cohort were lower in comparison to AS populations in other studies [13, 15]. A large T1 mapping data variability across different centers have been previously reported, influenced by differences in field strength, vendor-specific set-up and variations in sequences [34, 35]. Disparities in ECV values can also be expected with the non-uniformity of contrast agents and their doses [36]. Another explanation for such variability relates to differences in the study cohorts. When interpreting our results, we should consider that we examined relatively young, low-risk patients who were free from significant CAD, whereas other studies, especially those that included transcatheter treatment cohorts, enrolled patients who were in their 80 s and had a higher rate of comorbidities [37].

Study limitations

The study was composed of a small number of AS patients, however it included substantial number of myocardial biopsies. Due to the Covid-19 pandemic, delays in patient examinations and surgeries were experienced, causing uneven time frames between the preoperative patient assessment (echocardiographic and CMR) and surgery with myocardial sampling, potentially affecting the final result. Proportion of histologically measured myocardial fibrosis could have been affected by the size and depth of biopsy samples, as more superficially sampled and smaller biopsies may contain higher proportion of fibrotic tissue in comparison to larger biopsy samples. Although measuring T1 values only in the septum is a validated and common method, it might not represent the entire myocardium. Because we excluded patients with comorbidities, such as obstructive CAD, a history of myocardial infarction, renal failure and persistent atrial arrhythmias, our results should not be overgeneralized to the broader AS patient population. Another limitation of our study is that the increase in type I error across the statistical analyses was not controlled.

Conclusion

A comprehensive assessment of LV response to AS by integrating histology, CMR and STE reveals varying degrees of myocardial injury that are not apparent with traditional measures of LV systolic function. Histological myocardial fibrosis was associated with imaging and serum biomarkers of LV systolic dysfunction and left side chamber enlargement. We found that native T1 by CMR and GLS by STE differentiated patients with advanced cardiac remodelling, constituting a marker of subclinical cardiac damage. Of all imaging parameters, only GLS was associated with invasively and non-invasively measured myocardial fibrosis, demonstrating its potential as a surrogate marker of myocardial fibrosis.

Author contributions SG and PS are chief investigators; they conceived the study, led the proposal and protocol development. GB drafted the manuscript. PŠ, AA and TZ contributed to study implementation. NV and DP performed CMR scanning and data analysis. KR, VJ and AZ performed aortic valve replacement surgeries and sampled myocardial biopsies. EŽ and JB performed histological analysis. VS conceived and developed the statistical aspects of the study. All authors reviewed and approved the final version of the manuscript.

Funding Study is funded by the Research Council of Lithuania under 2014–2020 European Union investments in Lithuania operational program (09.3.3-LMT-K-712). The funder had no role in study design, execution, interpretation of the data, or decision to submit results.

Declarations

Conflict of interest The authors declare that they have no competing interests.

Ethical approval The study conformed to the principles of the Helsinki Declaration, and all subjects gave written consent to participate. The study (protocol, including qualitative and quantitative aspects, and trial materials, including patient information and consent form) was reviewed and approved by the Biomedical Research Ethics Committee of the Vilnius Region (16/March/2018; No: 158200-18/9-1014-558).

Consent to participate Informed consent was obtained from all individual participants included in the study.

Consent to publish The authors affirm that human research participants provided informed consent for publication of the images in Fig. 4.

References

1. Unverferth DV, Baker PB, Swift SE, Chaffee R, Fetters JK, Uretsky BF et al (1986) Extent of myocardial fibrosis and cellular hypertrophy in dilated cardiomyopathy. Am J of Cardiol 57(10):816–820. https://doi.org/10.1016/0002-9149(86)90620-x
2. Anderson KR, Sutton MG, Lie JT (1979) Histopathological types of cardiac fibrosis in myocardial disease. J Pathol 128(2):79–85. https://doi.org/10.1002/path.1711280205
3. Chin CWL, Everett RJ, Kwiecinski J, Vesey AT, Yeung E, Esson G et al (2017) Myocardial fibrosis and cardiac decompensation in aortic stenosis. JACC Cardiovasc Imaging 10:1320–1333
4. Dweck MR, Joshi S, Murigu T, Alpendurada F, Jabbour A, Melina G et al (2011) Midwall fibrosis is an independent predictor of mortality in patients with aortic stenosis. J Am Coll Cardiol 58:1271–1279
5. Villari B, Campbell SE, Hess OM, Mall G, Vassalli G, Weber KT et al (1993) Influence of collagen network on left ventricular systolic and diastolic function in aortic valve disease. J Am Coll Cardiol 22:1477–1484
6. Barone-Rochette G, Pierard S, Meester De, de Ravenstein C, Seldrum S, Melchior J, Maes F et al (2014) Prognostic significance of LGE by CMR in aortic stenosis patients undergoing valve replacement. J Am Coll Cardiol 64:144–154
7. Weidemann F, Herrmann S, Stork S, Niemann M, Frantz S, Lange V et al (2009) Impact of myocardial fibrosis in patients with symptomatic severe aortic stenosis. Circulation 120:577–584
8. Chin CW, Semple S, Malley T, White AC, Mirsadraee S, Weale PJ et al (2014) Optimization and comparison of myocardial T1 techniques at 3T in patients with aortic stenosis. Eur Heart J Cardiovasc Imaging 15:556–565
9. Balciunaite G, Skorniakov V, Rimkus A, Zaremba T, Palionis D, Valeviciene N et al (2020) Prevalence and prognostic value of late gadolinium enhancement on CMR in aortic stenosis: meta-analysis. Eur Radiol 30(1):640–651
10. Musa TA, Treibel TA, Vassiliou VS, Captur G, Singh A, Chin C et al (2018) Myocardial scar and mortality in severe aortic stenosis. Circulation 138(18):1935–1947. https://doi.org/10.1161/CIRCULATIONAHA.117.032839
11. Treibel TA, Kozor R, Schofield R, Benedetti G, Fontana M, Bhuva AN et al (2018) Reverse myocardial remodeling following valve replacement in patients with aortic stenosis. J Am Coll Cardiol 71:860–871
12. Everett RJ, Tastet L, Clavel MA, Chin CWL, Capoulade R, Vassiliou VS et al (2018) Progression of hypertrophy and myocardial fibrosis in aortic stenosis: a multicenter cardiac magnetic resonance study. Circ Cardiovasc Imaging 11:e007451
13. Everett RJ, Treibel TA, Fukui M, Lee H, Rigolli M, Singh A et al (2020) Extracellular myocardial volume in patients with aortic stenosis. J Am Coll Cardiol 75(3):304–316. https://doi.org/10.1016/j.jacc.2019.11.032
14. Chin CW, Pawade TA, Newby DE, Dweck MR (2015) Risk stratification in patients with aortic stenosis using novel imaging approaches. Circ Cardiovasc Imaging 8(8):e003421. https://doi.org/10.1161/CIRCIMAGING.115.003421
15. Park SJ, Cho SW, Kim SM, Ahn J, Carriere K, Jeong DS et al (2019) Assessment of myocardial fibrosis using multimodality imaging in severe aortic stenosis: comparison with histologic fibrosis. JACC Cardiovasc Imaging 12(1):109–119. https://doi.org/10.1016/j.jcmg.2018.05.028
16. Hwang IC, Kim HK, Park JB, Park EA, Lee W, Lee SP et al (2020) Aortic valve replacement-induced changes in native T1 are related to prognosis in severe aortic stenosis: T1 mapping cardiac magnetic resonance imaging study. Eur Heart J Cardiovasc Imaging 21(6):653–663. https://doi.org/10.1093/ehjci/jez201
17. Ng ACT, Prihadi EA, Antoni ML, Bertini M, Ewe SH, Ajmone Marsan N et al (2018) Left ventricular global longitudinal strain is predictive of all-cause mortality independent of aortic stenosis severity and ejection fraction. Eur Heart J Cardiovasc Imaging 19:859–867
18. Vahanian A, Beyersdorf F, Praz F, Milojevic M, Baldus S, Bauersachs J et al (2021) ESC/EACTS Scientific Document Group, 2021 ESC/EACTS Guidelines for the management of valvular heart disease: Developed by the Task Force for the management of valvular heart disease of the European Society of Cardiology (ESC) and the European Association for Cardio-Thoracic Surgery (EACTS). Eur Heart J. https://doi.org/10.1093/eurheartj/ehab395
19. Harris PA, Taylor R, Thielke R, Payne J, Gonzalez N, Conde JG (2009) Research electronic data capture (REDCap)-a metadata-driven methodology and workflow process for providing translational research informatics support. J Biomed Inform 42(2):377–381. https://doi.org/10.1016/j.jbi.2008.08.010
20. Lang RM, Badano LP, Mor-Avi V, Afilalo J, Armstrong A, Ernande L et al (2015) Recommendations for cardiac chamber quantification by echocardiography in adults: an update from the American Society of Echocardiography and the European Association of Cardiovascular Imaging. J Am Soc Echocardiogr 28:1–39
21. Baumgartner H, Hung J, Bermejo J, Chambers JB, Edvardsen T, Goldstein S et al (2017) Recommendations on the echocardiographic assessment of aortic valve stenosis: a focused update from the European Association of Cardiovascular Imaging and the American Society of Echocardiography. Eur Heart J Cardiovasc Imaging 8:254–275
22. Voigt JU, Pedrizzetti G, Lysyansky P, Marwick TH, Houle H, Baumann R et al (2015) Definitions for a common standard for 2D speckle tracking echocardiography: consensus document of the EACVI/ASE/Industry Task Force to standardize deformation imaging. Eur Heart J Cardiovasc Imaging 16:1–11
23. Taylor AJ, Salerno M, Dharmakumar R, Jerosch-Herold M (2016) T1 mapping: basic techniques and clinical applications. JACC Cardiovasc Imaging 9:67–81. https://doi.org/10.1016/j.jcmg.2015.11.005
24. Messroghli DR, Moon JC, Ferreira VM, Grosse-Wortmann L, He T et al (2017) Clinical recommendations for cardiovascular magnetic resonance mapping of T1, T2, T2* and extracellular volume: A consensus statement by the Society for Cardiovascular Magnetic Resonance (SCMR) endorsed by the European Association for Cardiovascular Imaging (EACVI). J Cardiovasc Magn Reson 19:75. https://doi.org/10.1186/s12968-017-0389-8
25. Ugander M, Oki AJ, Hsu LY, Kellman P, Greiser A, Aletras AH et al (2012) Extracellular volume imaging by magnetic resonance imaging provides insights into overt and sub-clinical myocardial pathology. Eur Heart J 33:1268–1278
26. Horai Y, Mizukawa M, Nishina H, Nishikawa S, Ono Y, Takemoto K et al (2019) Quantification of histopathological findings using a novel image analysis platform. J Toxicol Pathol 32(4):319–327. https://doi.org/10.1293/tox.2019-0022
27. R Core Team. R: A language and environment for statistical computing (2021) R Foundation for Statistical Computing, Vienna, Austria. R version 4.1.2 (2021–11–01) – "Bird Hippie". https://www.R-project.org/

28. Tanaka M, Fujiwara H, Onodera T, Wu DJ, Hamashima Y, Kawai C (1986) Quantitative analysis of myocardial fibrosis in normals, hypertensive hearts, and hypertrophic cardiomyopathy. Br Heart J 55(6):575–81. https://doi.org/10.1136/hrt.55.6.575
29. Treibel TA, López B, González A, Menacho K, Schofield RS, Ravassa S et al (2018) Reappraising myocardial fibrosis in severe aortic stenosis: an invasive and non-invasive study in 133 patients. Eur Heart J 39(8):699–709. https://doi.org/10.1093/eurheartj/ehx353
30. Galiuto L, Lotrionte M, Crea F, Anselmi A, Biondi-Zoccai GG, De Giorgio F et al (2006) Impaired coronary and myocardial flow in severe aortic stenosis is associated with increased apoptosis: a transthoracic Doppler and myocardial contrast echocardiography study. Heart 92(2):208–12. https://doi.org/10.1136/hrt.2005.062422
31. Hein S, Arnon E, Kostin S, Schon¨burg M, Elsa¨sser A, Polyakova V et al (2003) Progression from compensated hypertrophy to failure in the pressure-overloaded human heart: structural deterioration and compensatory mechanisms. Circulation 107(7):984–91
32. Kwak S, Everett RJ, Treibel TA, Yang S, Hwang D, Ko T et al (2021) Markers of myocardial damage predict mortality in patients with aortic stenosis. J Am Coll Cardiol 78:545–558. https://doi.org/10.1016/j.jacc.2021.05.047
33. Bull S, White SK, Piechnik SK, Flett AS, Ferreira VM, Loudon M et al (2013) Human non-contrast T1 values and correlation with histology in diffuse fibrosis. Heart 99(13):932–7. https://doi.org/10.1136/heartjnl-2012-303052
34. Vo HQ, Marwick TH, Negishi K (2020) Pooled summary of native T1 value and extracellular volume with MOLLI variant sequences in normal subjects and patients with cardiovascular disease. Int J Cardiovasc Imaging 36:325–336. https://doi.org/10.1007/s10554-019-01717-3
35. Kawel N, Nacif M, Zavodni A, Jones J, Liu S, Cibley CT et al (2012) T1 mapping of the myocardium: Intra-individual assessment of the effect of field strength, cardiac cycle and variation by myocardial region. J Cardiovasc Magn Reson 14(1):27. https://doi.org/10.1186/1532-429X-14-27
36. Dabir D, Child N, Kalra A, Rogers T, Gebker R, Jabbour A et al (2014) Reference values for healthy human myocardium using a T1 mapping methodology: results from the International T1 Multicenter cardiovascular magnetic resonance study. J Cardiovasc Magn Reson 16(1):69. https://doi.org/10.1186/s12968-014-0069-x
37. Puls M, Beuthner BE, Topci R, Vogelgesang A, Bleckmann A, Sitte M et al (2020) Impact of myocardial fibrosis on left ventricular remodelling, recovery, and outcome after transcatheter aortic valve implantation in different haemodynamic subtypes of severe aortic stenosis. Eur Heart J 41(20):1903–1914. https://doi.org/10.1093/eurheartj/ehaa033